

Full paper

Closed-loop control of compression paddle motion to reduce blurring in mammograms

AUTHORS AND AFFILIATIONS:

5 *Wang Kei Ma^a, David Howard^b, Peter Hogg^a

*corresponding author

Address correspondence to: Mr Wang Kei Ma. E-mail: carnby2000@gmail.com

a. Directorate of Radiography, University of Salford, Salford, UK, M5 4WT

b. School of Computing, Science & Engineering, University of Salford, Salford, UK, M5 4WT

10 Abstract

Background: Since the introduction of full field digital mammography (FFDM) a large number of UK breast cancer screening centers have reported blurred images, which can be caused by movement at the compression paddle during image acquisition.

15 Purpose: To propose and investigate the use of position feedback from the breast side of the compression paddle to reduce the settling time of breast side motion.

Method: Movement at the breast side of the paddle was measured using two calibrated linear potentiometers. A mathematical model for the compression paddle, machine drive and breast was developed using the paddle movement data. Simulation software was used to optimize the position

feedback controller parameters for different machine drive time constants and simulate the
20 potential performance of the proposed system.

Results: The results obtained are based on simulation alone and indicate that closed-loop control
of breast side paddle position dramatically reduced the settling time from over 90 seconds to less
than 4 seconds. The effect of different machine drive time constants on the open-loop response is
insignificant. With closed-loop control, the larger the time constant the longer the time required
25 for the breast side motion to settle.

Conclusions: Paddle motion induced blur could be significantly reduced by implementing the
proposed closed-loop control.

Keywords: Paddle motion, motion blurring, breast compression, closed-loop control, breast side
motion

30 **List of figure captions**

Figure 1: Alternative control systems for breast compression: a) using only machine side position
feedback; b) also using breast side position feedback.

Figure 2: Schematic diagram of the experimental setup

Figure 3: The simplest lumped parameter model of the paddle and breast

35 Figure 4: Models of the alternative control systems: a) conventional open-loop; b) closed-loop
using breast side position feedback.

Figure 5: Experimental data for paddle movement against time for the Selenia Dimensions 18x24
cm and 24x30 cm paddles

Figure 6: Experimental data for paddle movement against time for the Lorad Selenia 18x24 cm
40 and 24x30 cm paddles

Figure 7: The step responses of the Selenia Dimensions open-loop breast compression system for
machine drive time constants (τ) of 0.1s, 0.2s and 0.4s (i.e. without breast side position
feedback). The upper group of curves (τ_1 - τ_3) are for the 24x30 cm paddle and the lower group
of curves (τ_4 - τ_6) are for the 18x24 cm paddle. Note that the differences between the three
45 responses for each paddle are negligible.

Figure 8: The step responses of the Lorad Selenia open-loop breast compression system for
machine drive time constants (τ) of 0.1s, 0.2s and 0.4s (i.e. without breast side position
feedback). The upper group of curves (τ_1 - τ_3) are for the 24x30 cm paddle and the lower group
of curves (τ_4 - τ_6) are for the 18x24 cm paddle. Note that the differences between the three
50 responses for each paddle are negligible.

Figure 9: The step responses of the Selenia Dimensions closed-loop breast compression system
for machine drive time constants (τ) of 0.1s, 0.2s and 0.4s (i.e. with breast side position
feedback). The curves labelled τ_1 - τ_3 are for the 24x30 cm paddle and the curves labelled τ_4 - τ_6
are for the 18x24cm paddle.

55 Figure 10: The step responses of the Lorad Selenia closed-loop breast compression system for
machine drive time constants (τ) of 0.1s, 0.2s and 0.4s (i.e. with breast side position feedback).
The curves labelled τ_1 - τ_3 are for the 24x30 cm paddle and the curves labelled τ_4 - τ_6 are for the
18x24cm paddle.

60 **Notation**

	c_b	Breast viscous friction coefficient
	c_m	Motor viscous friction coefficient
	C_1 and C_2	Arbitrary constants which depend on initial conditions at the start of the movement
	$G_{drive}(s)_{CL}$	Machine drive closed-loop transfer function
65	$G_{drive}(s)_{OL}$	Machine drive open-loop transfer function
	G_{dyn}	Paddle and breast 2 nd order dynamics
	G_{gain}	Paddle and breast steady-state gain
	G_{PID}	PID controller transfer function
	G_{sys}	Paddle and breast transfer function
70	J_m	The machine's effective inertia
	k_b	Breast spring constant
	k_c	Proportional gain for the machine drive control
	k_m	Motor gain
	k_p	Paddle spring constant
75	k_{prop}	Proportional gain of the PID controller
	k_{integ}	Integral gain of the PID controller
	k_{deriv}	Derivative gain of the PID controller
	m_b	Effective mass of the breast and paddle
	R	Ratio between linear velocity of the paddle (\dot{x}_m) and motor angular velocity ($\dot{\theta}_m$)
80	s	The Laplace variable
	T_m	Motor torque
	x_m	Machine side paddle position

	x_p	Breast side paddle position
	$x_{p_{ss}}$	Steady-state breast side paddle position
85	τ	Machine drive time constant
	ω_n	System natural frequency
	ζ	System damping ratio
	$\dot{\theta}_m$	Motor angular velocity
	λ_1 and λ_2	Empirically identified exponents that describe the motion of the paddle.
90		

1. Introduction

Since the introduction of full field digital mammography (FFDM) a large number of UK breast cancer screening centers have identified blurred images during local audit; however, few reports have been published about the causes and possible solutions^{1,2}. Blurring can be caused by a number of factors including inadequate breast compression, long exposures and patient movement³. Studies have also shown that image blurring can be caused by movement of the compression paddle during image acquisition^{4,5,6}. Previous research into paddle motion has demonstrated that the settling time required for the compression paddle motion to become negligible is approximately 30 seconds and most of the movement occurs within the first 10 seconds, which is when the mammography image would normally be formed⁶.

Current breast compression systems control the position of the machine side of the paddle (i.e. the side on which it is attached to the machine) and, if position feedback is used, it is feedback from the machine side (e.g. in the manner shown in Figure 1a). Therefore, even if the machine side motion settles quickly, there is no guarantee that the remainder of the paddle and breast do not

105 continue to move during image acquisition causing motion blurring. In light of this and building
on the work of Ma et al⁶ on paddle movement, we propose a new feedback control system with
the aim of minimizing the settling time of the paddle as a whole and, hence, the breast. Referring
to Figure 1b, we propose the use of position feedback from the breast side of the paddle (the right-
hand side in Figure 2) so that the machine drive is controlled in such a manner that the breast side
110 motion settles quickly. This relies on the assumption that this better reflects breast motion as a
whole because, when the machine side is stationary, any change in compressed breast thickness
and shape will change the amount of paddle-bend and hence the position of the breast side of the
paddle.

Referring to Figure 1b, in the proposed solution, a proportional, integral and derivative (PID)
115 controller is driven by the error in breast side paddle position. The PID controller determines the
set-point for the machine side position control (inner feedback loop). PID controllers are
commonly used when a fast settling time is required and can be tuned to deal with variability in
the plant transfer function⁹ (see footnote). This is important in this application because female
breasts vary widely in terms of size, compressed thickness and density and, hence, the plant (breast)
120 transfer function will vary from woman to woman.

Footnote: The transfer function of a linear system is defined as the ratio of the Laplace transform of the
output variable to the Laplace transform of the input variable. It is an input-output description of the
behavior of a system with all initial conditions assumed to be zero⁷. Transfer functions are widely used in
125 the study of dynamic control systems because they are algebraic functions rather than differential equations,
which makes the analysis simpler⁸.

In this paper we present the results of a simulation study to demonstrate the potential performance of the proposed system and, in particular, the benefits associated with using feedback of the breast side paddle position.

130

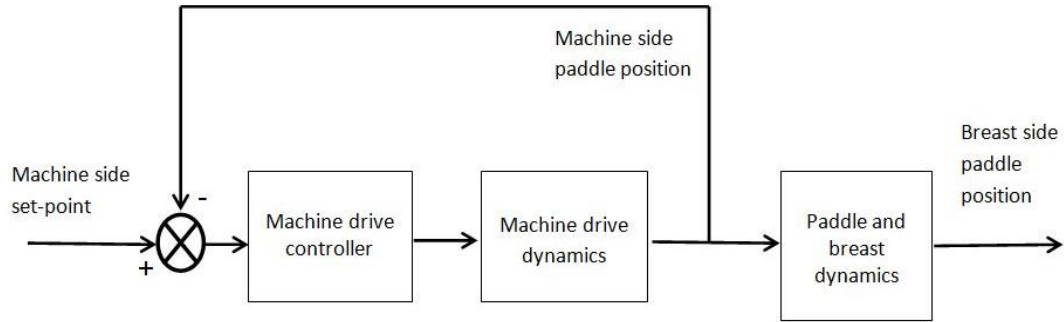


Figure 1a

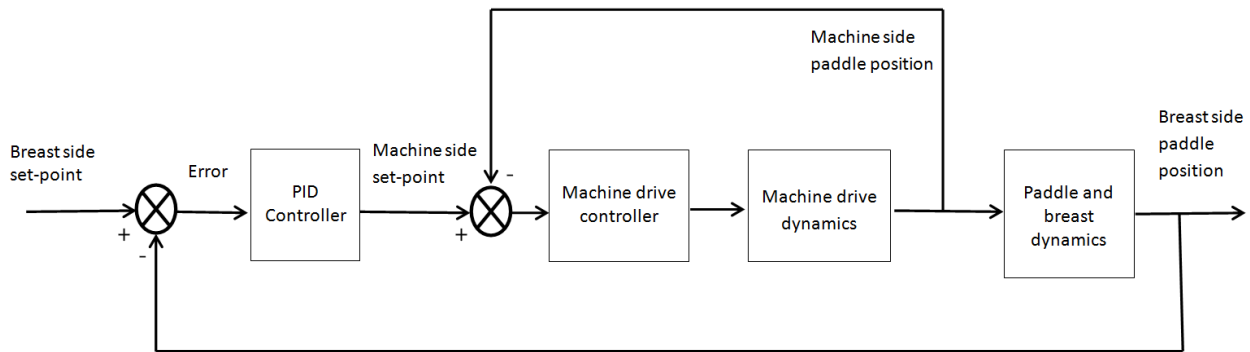


Figure 1b

Figure 1: Alternative control systems for breast compression: a) using only machine side position feedback; b) also using breast side position feedback.

2. Methods

135 2.1 Measurement of paddle movement

A Selenia Dimensions mammography unit (*Hologic Incorporated, Bedford, MA, USA*) and a Lorad Selenia mammography unit (*Hologic Incorporated, Bedford, MA, USA*) were used in this study, fitted with either an 18x24 cm or a 24x30 cm compression paddle. Routine equipment quality assurance (QA) was performed and the results complied with the manufacturer specifications¹⁰. A
 140 deformable breast phantom (*Trulife, Sheffield, United Kingdom*) with compression characteristics similar to a female breast¹¹ was compressed manually to approximately 80 N, after which the movement of the breast side of the paddle was recorded at 0.5 second intervals for 90 seconds. The machine side of the paddle was stationary during measurement. The movement of the breast side of the paddle was measured using two calibrated linear potentiometers (Activesensors, Dorset,
 145 United Kingdom). Figure 2 shows the experimental setup. The measurement was repeated three times to minimize the experimental uncertainties.

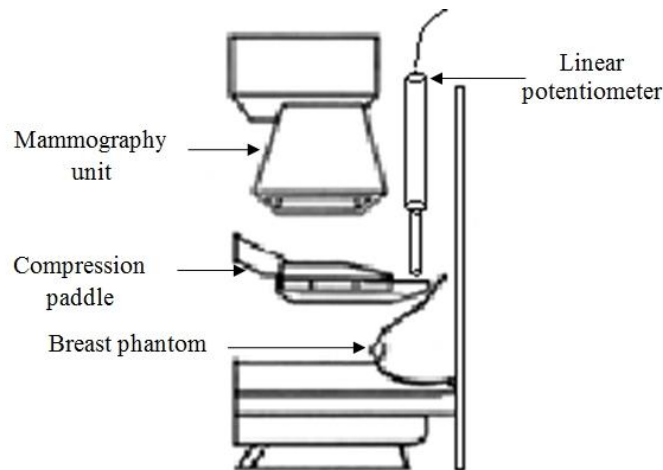


Figure 2: Schematic diagram of the experimental setup

2.2 Modeling the paddle and breast

Previous work by the authors⁶ suggests that the paddle motion is that of either a 1st order system
 150 or an over-damped 2nd order system. This is also supported by the data presented in this study. To

the more appropriate of these two models, the simplest lumped parameter model was considered as shown in Figure 3. The breast is represented as being viscoelastic (c_b and k_b). The effective mass of the breast and paddle is represented by m_b . The paddle is represented by the spring k_p . In this model x_m is the machine side paddle position and x_p is the breast side paddle position.

155 Applying Newton's 2nd law we obtain:

$$k_p(x_m - x_p) - k_b x_p - c_b \dot{x}_p = m_b \ddot{x}_p \quad (1)$$

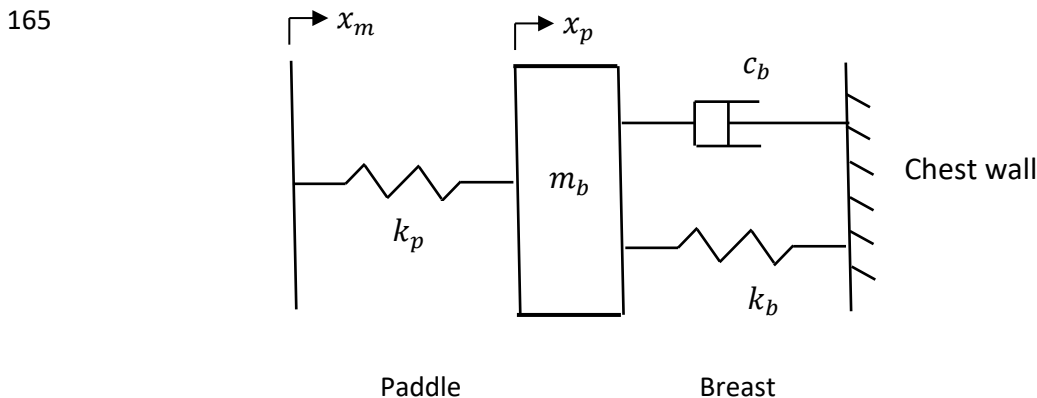
where the three terms on the left of the equation are the paddle elastic force, the breast elastic force, and the breast viscous force respectively. Rearranging equation 1 we obtain:

$$m_b \ddot{x}_p + c_b \dot{x}_p + (k_p + k_b)x_p = k_p x_m \quad (2)$$

160 Therefore we adopted an over-damped 2nd order model of the paddle and breast. Furthermore, equation 2 can be written in standard form as follows:

$$\ddot{x}_p + 2\zeta \omega_n \dot{x}_p + \omega_n^2 x_p = \frac{k_p}{(k_p + k_b)} \omega_n^2 x_m \quad (3)$$

Where $\zeta = \frac{c_b}{2\sqrt{(k_p + k_b)m_b}}$ is the system's damping ratio and $\omega_n = \sqrt{\frac{(k_p + k_b)}{m_b}}$ is the system's natural frequency.



170 *Figure 3: The simplest lumped parameter model of the paddle and breast.*

Because the machine side of the paddle was stationary during our experimental measurements, the resulting motion represents the transient response only (i.e. there was no forcing function). This transient motion of the paddle and breast is the solution to the following homogeneous (or
175 complementary) equation¹²:

$$\ddot{x}_p + 2\zeta\omega_n\dot{x}_p + \omega_n^2x_p = 0 \quad (4)$$

Where ω_n is the system's natural frequency and ζ is its damping ratio

For over-damped 2nd order dynamics, the general solution to equation 4 is given by:

$$x_p(t) = C_1e^{\lambda_1t} + C_2e^{\lambda_2t} \quad (5)$$

180 Where the two exponents are given by:

$$\lambda_{1,2} = -\zeta\omega_n \pm \omega_n\sqrt{\zeta^2 - 1} \quad (6)$$

And C_1 and C_2 are arbitrary constants that depend on the initial conditions of the system at the start of the movement. The four constants in equation 5 were identified using the experimental motion data and the Mathworks curve fitting tool, which minimizes the sum of the square errors. The two
185 values found for λ_1 and λ_2 were substituted in equations 6, which were then solved to find ω_n and ζ .

Laplace transforming both sides of equation 3 and solving for the transfer function⁹ we obtain:

$$G_{\text{sys}}(s) = \frac{x_p}{x_m} = \frac{k_p}{(k_b+k_p)} \frac{\omega_n^2}{s^2+2\zeta\omega_n s+\omega_n^2} \quad (7)$$

190 Where $G_{\text{sys}}(s)$ is the paddle and breast transfer function, with the breast side paddle position (x_p) as output, the machine side paddle position (x_m) as input, and where s is the Laplace variable. Considering equation 7, it is clear that the model of the paddle and breast can be divided into two parts representing: a) a steady-state gain (obtained by substituting $s = 0$); and b) the 2nd order dynamics. These two parts have the following transfer functions:

$$195 \quad G_{\text{gain}} = \frac{x_{p_{ss}}}{x_m} = \frac{k_p}{(k_b+k_p)}$$

$$G_{\text{dyn}}(s) = \frac{x_p}{x_{p_{ss}}} = \frac{\omega_n^2}{s^2+2\zeta\omega_n s+\omega_n^2}$$

Where $x_{p_{ss}}$ is the steady-state breast side paddle position. This assumes the breast has a linear elastic relationship which is unlikely. Furthermore, we have adopted an estimate of $G_{\text{gain}} = 0.9$ (i.e. we assume the paddle is much stiffer than the breast). However, these assumptions have little
200 impact on the conclusions of this study as we are primarily concerned with the dynamics ($G_{\text{dyn}}(s)$), the parameters of which (ζ and ω_n) we can determine from our experimental data as described above.

2.3 Modeling the machine drive

Our aim here was to develop the simplest model of the machine drive that would allow us to
205 compare the open-loop and closed-loop alternatives shown in Figure 1. Assuming that changes in the motor torque (T_m) propelling the machine drive can occur very quickly, and that the motor

torque overcomes viscous friction (c_m) and accelerates the machine's effective inertia (J_m), as seen by the motor, it can be shown that the following equation of motion applies:

$$J_m \ddot{\theta}_m + c_m \dot{\theta}_m = T_m \quad (8)$$

210 As a first approximation, if we neglect the acceleration term and include the ratio (R) between the linear velocity of the paddle (\dot{x}_m) and the motor angular velocity ($\dot{\theta}_m$), this simplifies equation 8 to $\dot{x}_m = k_m T_m$, where $k_m = R/c_m$. This leads to the following open-loop transfer function for the machine drive:

$$G_{drive}(s)_{OL} = \frac{x_m}{T_m} = \frac{k_m}{s} \quad (9)$$

215 If we assume simple closed-loop proportional control (with gain k_c), then the transfer function is given by⁹:

$$G_{drive}(s)_{CL} = \frac{x_m}{x_{m_{setpoint}}} = \frac{k_c k_m / s}{1 + k_c k_m / s} = \frac{1}{1 + \tau s} \quad (10)$$

where the time constant $\tau = 1/k_c k_m$. Although a more complex model of the machine drive could be used, for our purposes we simply needed to model the machine drive's speed of response, which
 220 is determined by the time constant. Because we don't have experimental data for machine drive response and also because it will differ between machine suppliers, we have included simulation results for a range of time constants to show the effect of different machine drive dynamics.

2.4 Controller modeling and design

Referring to Figure 4, we considered two scenarios: a) conventional control where the motion of
 225 the breast side of the paddle is controlled in an open-loop manner; and b) closed-loop PID control
 using position feedback from the breast side of the paddle.

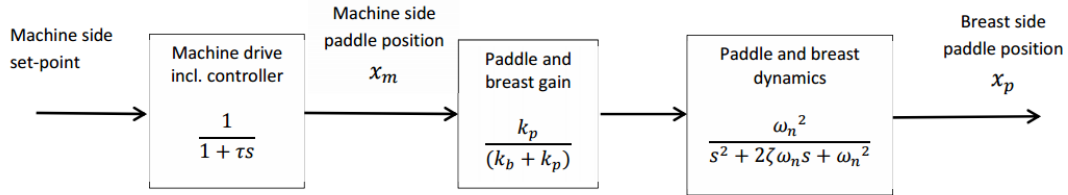


Figure 4a

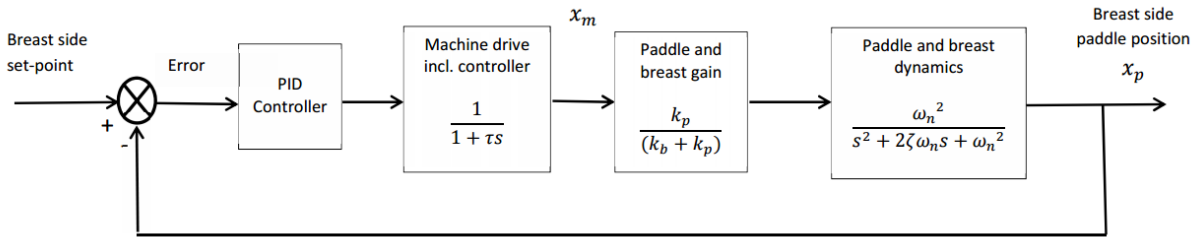


Figure 4b

Figure 4: Models of the alternative control systems: a) conventional open-loop; b) closed-loop using breast side position feedback.

Both scenarios were modeled in Mathworks Simulink and the PID controller parameters tuned to
 minimize the settling time of the breast side paddle motion. For the purposes of this study, in both
 230 scenarios we compare the system responses with machine drive time constants (τ) of 0.1s, 0.2s
 and 0.4s to determine the importance of machine drive response. In this context, $\tau = 0.4s$ is
 considered a conservative value, corresponding to a 95% rise time of 1.2 seconds and hence not
 requiring a fast servo-system. The transfer function of the PID controller is given by:

$$G_{PID} = k_{prop} + k_{integ} \frac{1}{s} + k_{deriv} s \quad (11)$$

235 Where k_{prop} is the proportional gain, k_{integ} is the integral gain, and k_{deriv} is the derivative gain.
 The PID controller was tuned using the Mathworks Simulink response optimization tool to
 minimize the integral square error and also satisfy the constraint that the overshoot should be zero
 (because overshoot might cause breast pain).

3. Results

240 3.1 Experimental data and model fitting

As we expected, the paddle movement on the breast side decreased in an over-damped 2nd order
 manner and took approximately 80 seconds to settle (Figures 5 and 6).

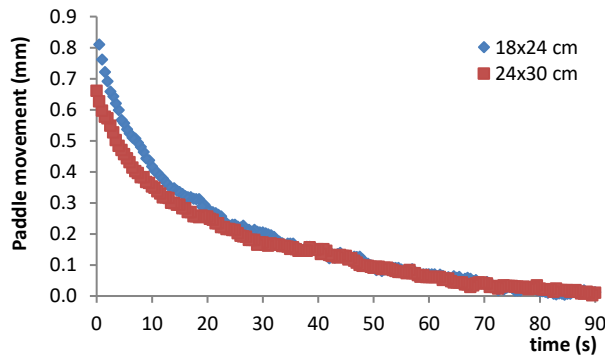


Figure 5: Experimental data for paddle movement against time for the Selenia Dimensions 18x24 cm and 24x30 cm paddles

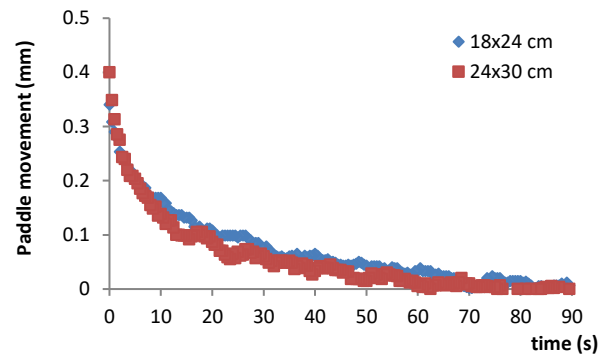


Figure 6: Experimental data for paddle movement against time for the Lorad Selenia 18x24 cm and 24x30 cm paddles

Using the curve fitting method described previously, this data was used to derive the following
 245 equations for the motion of the Selenia Dimensions and Lorad Selenia 18x24 cm and 24x30 cm
 paddles.

$$x_{p\ 18x24cm\ Selenia}(t) = 0.58e^{-0.036t} + 0.27e^{-0.28t} \quad (12)$$

$$x_{p\ 24x30cm\ Selenia}(t) = 0.48e^{-0.034t} + 0.18e^{-0.27t} \quad (13)$$

$$x_{p\ 18x24cm\ Lorad}(t) = 0.22e^{-0.036t} + 0.11e^{-0.39t} \quad (14)$$

250 $x_{p\ 24x30cm\ Lorad}(t) = 0.21e^{-0.045t} + 0.16e^{-0.32t} \quad (15)$

The coefficients of correlation (R-squared) for the Selenia Dimensions and Lorad Selenia paddles are listed in table 1.

Table 1: Coefficients of correlation (R-squared) for Selenia Dimensions and Lorad Selenia paddles

255

Mammography machine	Selenia Dimensions		Lorad Selenia	
Paddle size	18x24 cm	24x30 cm	18x24 cm	24x30 cm
R-squared	0.9968	0.9943	0.9874	0.9864

The two exponents in equations 12 to 15 were then used to solve for the natural frequency (ω_n) and damping ratio (ζ) of the paddle and breast. For the Selenia Dimensions paddles ω_n and ζ were found to be 0.101 rad/s and 1.565 respectively for the 18x24 cm paddle; and 0.096 rad/s and 1.591 respectively for the 24x30 cm paddle. For the Lorad Selenia paddles ω_n and ζ were found to be 0.117 rad/s and 1.799 respectively for the 18x24 cm paddle; and 0.121 rad/s and 1.531 respectively for the 24x30 cm paddle. Hence, the transfer functions for the Selenia Dimensions and Lorad Selenia paddles and breast are given by:

$$G_{dyn}(s)_{18x24cm\ Selenia} = \frac{x_P}{x_{PSS}} = \frac{0.0102}{s^2 + 0.3168s + 0.0102} \quad (16)$$

265 $G_{dyn}(s)_{24x30cm\ Selenia} = \frac{x_P}{x_{PSS}} = \frac{0.0092}{s^2 + 0.3049s + 0.0092} \quad (17)$

$$G_{dyn}(s)_{18x24cm\ Lorad} = \frac{x_P}{x_{PSS}} = \frac{0.0138}{s^2 + 0.4223s + 0.0138} \quad (18)$$

$$G_{dyn}(s)_{24x30cm\ Lorad} = \frac{x_P}{x_{PSS}} = \frac{0.0146}{s^2 + 0.3697s + 0.0146} \quad (19)$$

3.2 Controller performance

Using the Mathworks Simulink response optimization tool, PID controller gains for the Selenia
270 Dimensions and Lorad Selenia 18x24 cm and 24x30 cm paddles were established for both
scenarios (open-loop and closed-loop using breast side position feedback) and also for machine
drive time constants (τ) of 0.1s, 0.2s and 0.4s. The PID gains and corresponding step responses
for the open-loop and closed-loop systems are shown in Tables 2 and 3 and Figures 7 to 10.

Referring to Tables 2 and 3 and Figures 7 and 8, for each paddle, the open-loop step response
275 curves for all machine drive time constants overlay one another as there are no
significant differences between the curves. In other words, the effect of different machine drive
time constants on the open-loop response is insignificant. However, there is a small difference
between the two paddle sizes; but in both cases the settling time is very long.

Referring to Tables 2 and 3 and Figures 9 and 10, closed-loop control of breast side paddle position
280 dramatically reduces the settling time from over 90 seconds to less than 4 seconds for a machine
drive time constant of 0.4s. Furthermore, the smaller the machine drive time constant, the shorter
the rise and settling times; but this effect is not as important as switching to closed-loop control in
the first place. Although there are small differences between the two paddle sizes, these do not
alter the observed trends or the conclusions drawn.

285

Table 2: PID controller gains and step response performance for Selenia Dimensions 18x24 cm and 24x30 cm paddles

	Machine drive time constant (τ)											
	Open-loop system						Closed-loop system					
	24x30 cm			18x24 cm			24x30 cm			18x24 cm		
	$\tau_1=0.1$	$\tau_2=0.2$	$\tau_3=0.4$	$\tau_4=0.1$	$\tau_5=0.2$	$\tau_6=0.4$	$\tau_1=0.1$	$\tau_2=0.2$	$\tau_3=0.4$	$\tau_4=0.1$	$\tau_5=0.2$	$\tau_6=0.4$
k_{prop}	-	-	-	-	-	-	91.96	51.39	25.99	100.77	49.66	27.11
k_{integ}	-	-	-	-	-	-	2.75	1.54	0.79	3.28	1.61	0.88
k_{deriv}	-	-	-	-	-	-	304.89	168.35	85.27	329.63	158.43	86.26
10-90% rise time	65.68	65.68	65.69	61.03	61.04	61.05	0.67	1.18	2.32	0.53	1.12	2.01
98% settling time	119.44	119.54	119.74	111.03	111.13	111.33	1.16	1.98	3.89	0.89	1.87	3.27

Table 3: PID controller gains and step response performance for Lorad Selenia 18x24 cm and 24x30cm paddles

	Machine drive time constant (τ)											
	Open-loop system						Closed-loop system					
	24x30 cm			18x24 cm			24x30 cm			18x24 cm		
	$\tau_1=0.1$	$\tau_2=0.2$	$\tau_3=0.4$	$\tau_4=0.1$	$\tau_5=0.2$	$\tau_6=0.4$	$\tau_1=0.1$	$\tau_2=0.2$	$\tau_3=0.4$	$\tau_4=0.1$	$\tau_5=0.2$	$\tau_6=0.4$
k_{prop}	-	-	-	-	-	-	42.78	33.13	22.26	98.20	51.55	28.41
k_{integ}	-	-	-	-	-	-	1.69	1.31	0.90	3.20	1.73	0.95
k_{deriv}	-	-	-	-	-	-	114.61	89.30	61.30	232.03	123.28	69.04
10-90% rise time	49.78	49.78	49.78	62.11	62.11	62.10	1.24	1.45	2.00	0.56	1.06	1.87
98% settling time	90.60	90.70	90.90	112.65	112.75	112.95	2.22	2.55	3.26	0.94	1.74	3.01

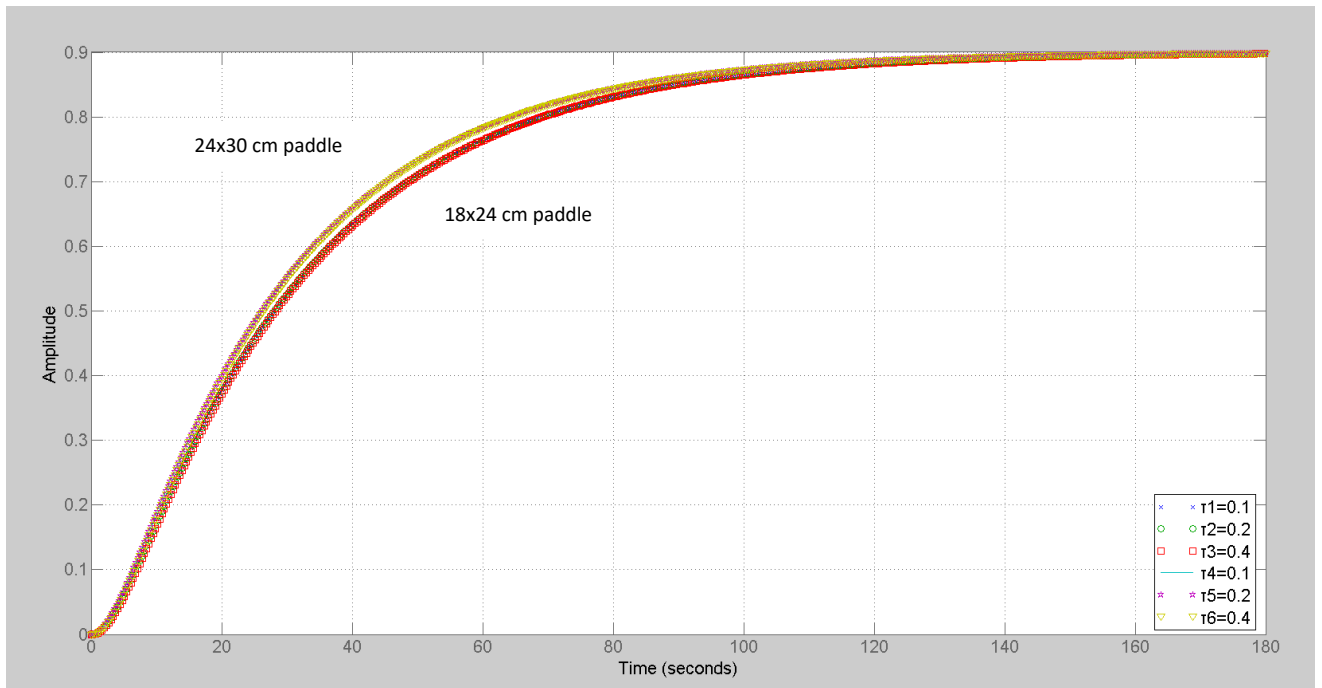


Figure 7: The step responses of the Selenia Dimensions open-loop breast compression system for machine drive time constants (τ) of 0.1s, 0.2s and 0.4s (i.e. without breast side position feedback). The upper group of curves (τ_1 - τ_3) are for the 24x30 cm paddle and the lower group of curves (τ_4 - τ_6) are for the 18x24 cm paddle. Note that the differences between the three responses for each paddle are negligible.

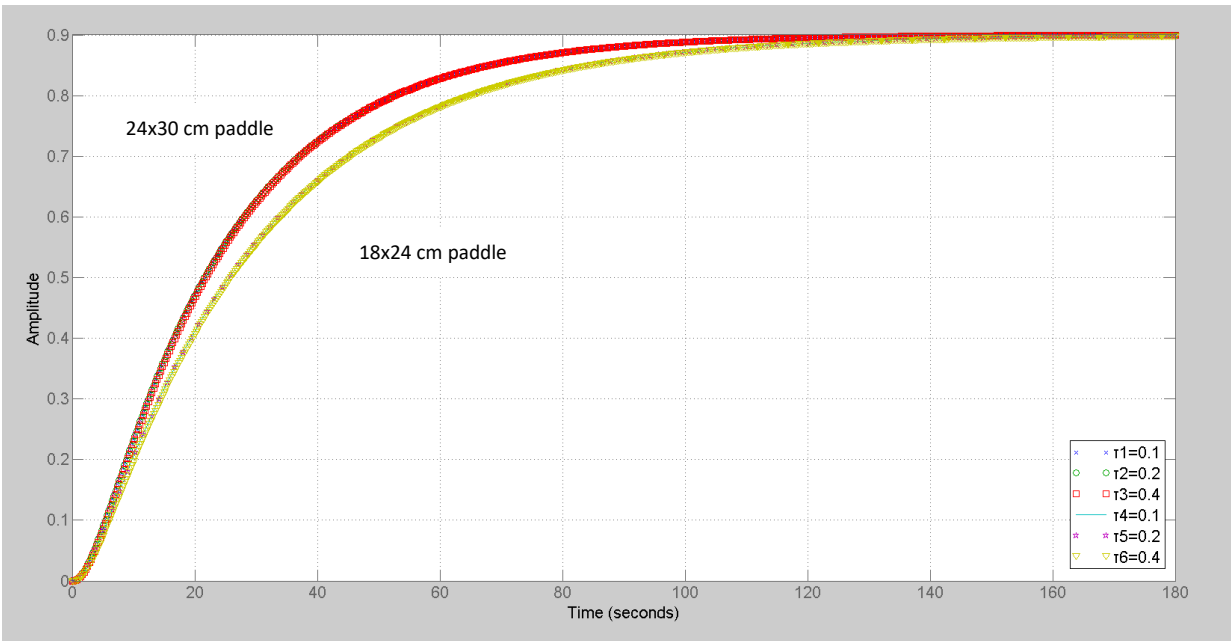


Figure 8: The step responses of the Lorad Selenia open-loop breast compression system for machine drive time constants (τ) of 0.1s, 0.2s and 0.4s (i.e. without breast side position feedback). The upper group of curves (τ_1 - τ_3) are for the 24x30 cm paddle and the lower group of curves (τ_4 - τ_6) are for the 18x24 cm paddle. Note that the differences between the three responses for each paddle are negligible.

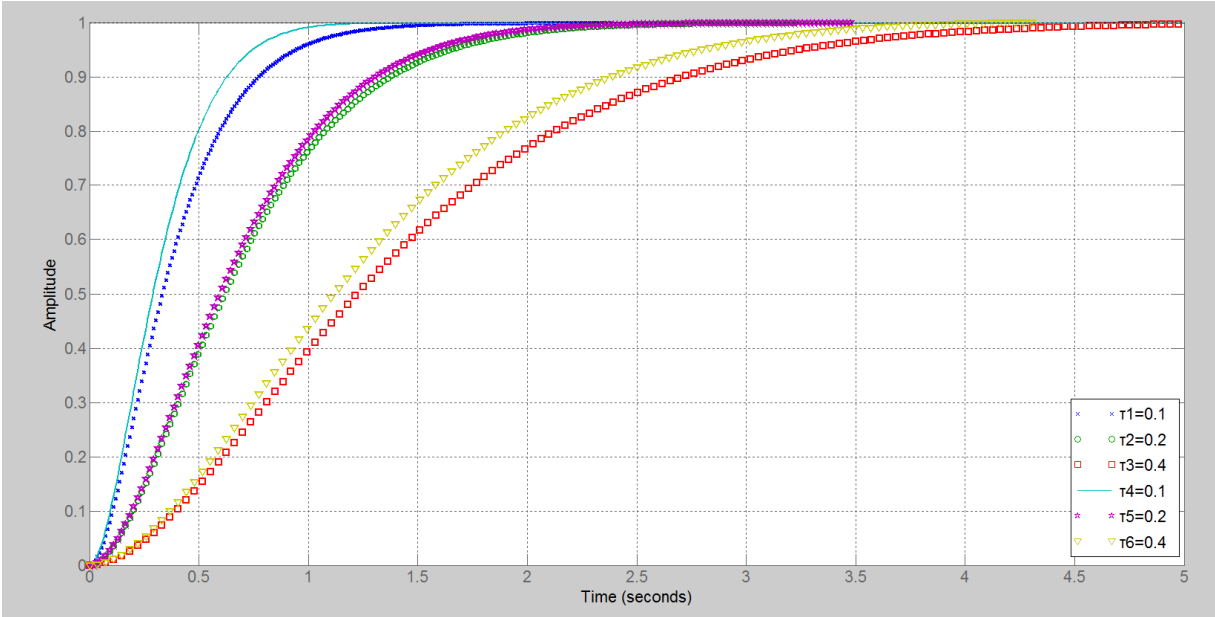


Figure 9: The step responses of the Selenia Dimensions closed-loop breast compression system for machine drive time constants (τ) of 0.1s, 0.2s and 0.4s (i.e. with breast side position feedback). The curves labelled $\tau 1$ - $\tau 3$ are for the 24x30 cm paddle and the curves labelled $\tau 4$ - $\tau 6$ are for the 18x24 cm paddle.

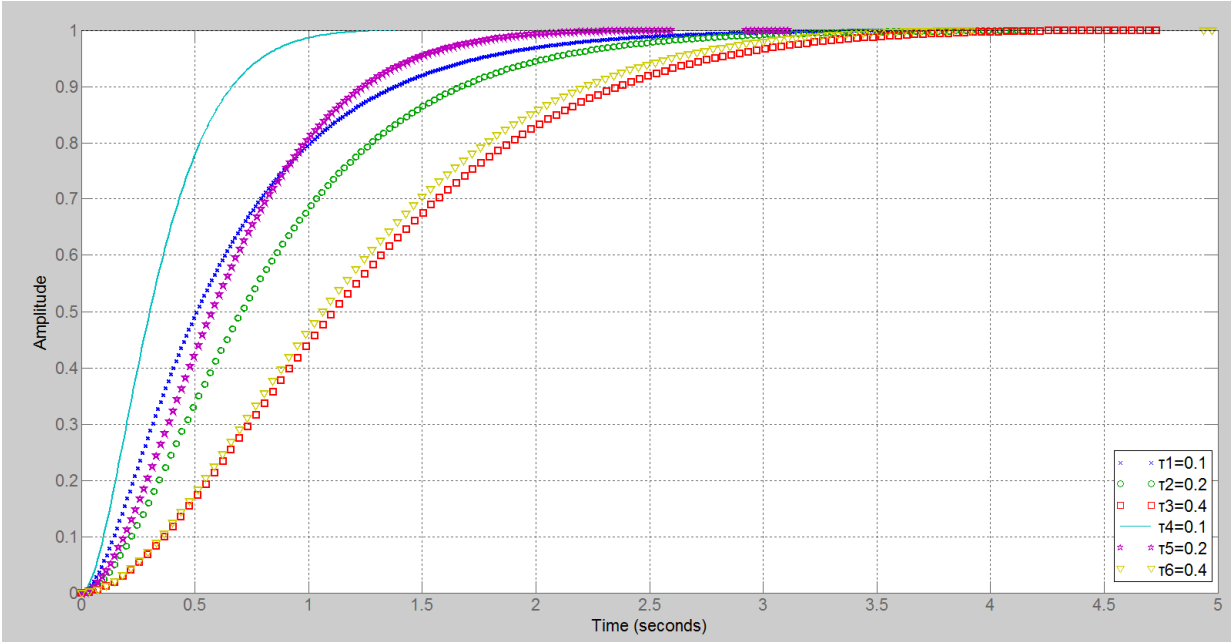


Figure 10: The step responses of the Lorad Selenia closed-loop breast compression system for machine drive time constants (τ) of 0.1s, 0.2s and 0.4s (i.e. with breast side position feedback). The curves labelled $\tau 1$ - $\tau 3$ are for the 24x30 cm paddle and the curves labelled $\tau 4$ - $\tau 6$ are for the 18x24 cm paddle.

4. Discussion

4.1 Clinical implications of the results

300 Current breast compression systems use open-loop control of breast side paddle position and, referring to Tables 2 and 3, our simulation results indicate a settling time of almost 2 minutes. This means that it is highly likely that there will still be paddle movement during image acquisition, which could cause blurring of the mammogram. Conversely, we have shown that closed-loop control of breast side paddle position dramatically reduces the settling time to less than 4 seconds
305 (even for a slow machine drive where $\tau = 0.4s$). Therefore, it is possible that paddle motion induced blur could be significantly reduced by implementing the proposed closed-loop control of breast side paddle position.

4.2 Study limitations

This preliminary study is based on simulation alone and the results will need to be validated against
310 in-vivo measurements taken during mammogram acquisition. However, this would require a physical prototype of a closed-loop controller using breast side paddle position feedback. The aim of the simulation study reported here was to justify the creation of such a prototype for the next stage of our work. Furthermore, we assume that the motion of the breast side of the paddle reflects breast motion as a whole. Again, physical prototyping and an experimental study would be
315 required to confirm this.

A simple machine drive model was used in this study and this was not validated against experimental results. However, it can be reasonably assumed that the response of the machine

drive will be much faster than that of the paddle and breast (e.g. a machine drive time constant of 0.4s or less). This means that changes in the machine drive dynamics have only a small effect compared to the dramatic reduction in settling time (over 80 seconds) achieved by using closed-loop control and, therefore, such changes do not alter the overall conclusions of this study. We have included results for three different machine drive time constants to demonstrate this.

The breast and paddle model used in this study is a simplified linear model. In reality, the breast is likely to have non-linear visco-elastic characteristics. However, the experimental results shown in Figures 5 and 6 support our decision to approximate the dynamic response (G_{dyn}) to that of a linear 2nd order system. The steady-state gain ($G_{gain} = 0.9$) is less relevant in the context of settling time and changing its value would not alter the results as the PID gains would simply change accordingly.

In practice, female breasts vary widely in terms of size, compressed thickness and density (which depends on the mix of glandular and fatty tissues) and, hence, the plant (breast) transfer function will vary from woman to woman. Therefore, the proposed closed-loop controller would have to be able to deal with this. It may be possible to tune the PID controller so that it is robust to this variability in the plant transfer function. If this is not possible, then adaptive control techniques could be investigated. In adaptive control, the controller gains are automatically adjusted to suit different system dynamics (breast characteristics in this case). These could be based on a gain scheduling approach that uses fixed look-up tables that define how the controller gains should vary as a function of certain system parameters (breast characteristics). Alternatively, an automatic model estimation approach could be adopted using sensor data captured during breast compression.

5. Conclusions

340 Paddle motion induced blur could be significantly reduced by implementing the proposed closed-loop control of breast side paddle position. With a machine drive time constant of 0.4s, the settling time is reduced from over 90 seconds for the open-loop system to less than 4 seconds for the closed-loop system. Reducing the machine drive time constant further reduces the settling time of the closed-loop system, but this effect is not as important as switching to closed-loop control in
 345 the first place. Although there are small differences between the two paddle sizes, these do not alter the observed trends or the conclusions drawn.

Conflict of interest statement:

The authors have no conflict of interest.

References

- 350 ¹P.Hogg, K.Szczepura, J.Kelly and J.Taylor, "Blurred digital mammography images," *Radiography*.**18**, 55–56 (2012).
- ²P.Hogg, J.Kelly, S.Millington, C.Willcock, G.McGeever and S.Tinston, et al., "Paddle motion analysis," East of England Conference, Cambridge, UK. National Health Service Breast Screening Programme, (2012).
- 355 ³D.Seddon, K.A.Schofield and C.A.Waite, "Investigation into possible causes of blurring in mammograms," *Breast Cancer Res.***2(suppl2)**, A64(2000).doi: 10.1186/bcr253
- ⁴W.K. Ma, R.Aspin, J.Kelly, S. Millington and P.Hogg, "What is the minimum amount of simulated breast movement required for visual detection of blurring? An exploratory
 360 investigation." *Br J Radiol.***88**, 20150126 (2015).doi: 10.1259/bjr.20150126
- ⁵W.K.Ma, P.Hogg, J.Kelly and S.Millington. "A method to investigate image blurring due to mammography machine compression paddle movement," *Radiography*.**21**, 36-41.(2015).doi:10.1016/j.radi.2014.06.004
- ⁶W.K.Ma, D.Brettell, D.Howard, J.Kelly, S.Millington and P. Hogg. "Extra patient movement during mammographic Imaging: An Experimental Study," *Br J Radiol.***87**, 20140241. (2014).doi: 10.1259/bjr.20140241
- 365 ⁷R. C. Dorf and R. H. Bishop, *Modern Control Systems*, 12th ed.(Pearson, London, 2010)

- 370 ⁸CW de Silva, *Modeling and Control of Engineering Systems*, 1st ed.(CRC Press , Boca Raton ,2009)
- ⁹G.F.Franklin, J.D.Powell and A.E.Naeini, *Feedback Control of Dynamic System*, 7th ed.(Pearson, London, 2014)
- 375 ¹⁰A.C.Moore, D.R.Dance, D.S.Evans, C.P.Lawinski, E.M.Pitcher and A.Rust, et al., *The Commissioning and Routine Testing of Mammographic X-Ray Systems: A Technical Quality Control Protocol*, Report No. 89(IPEM, York, 2005)
- ¹¹I.Hauge, P.Hogg, K.Szczepura, P. Connolly, G.McGill and C.Mercer. “The readout thickness versus the measured thickness for a range of screen film mammography and full field digital mammography units”, *Med.Phys.***39**(1), 263–271 (2012).
- 380 ¹² D. Zill, W. Wright, *Advanced Engineering Mathematics*, 5th ed.(Jones & Bartlett Learning, London, 2012)